

## Damping in Yttrium Iron Garnet Nanoscale Films Capped by Platinum

Yiyan Sun, Houchen Chang, Michael Kabatek, Young-Yeal Song, Zihui Wang, Michael Jantz,  
William Schneider, and Mingzhong Wu\*

*Department of Physics, Colorado State University, Fort Collins, Colorado 80523, USA*

E. Montoya, B. Kardasz, and B. Heinrich

*Physics Department, Simon Fraser University, Burnaby, British Columbia, V5A 1S6, Canada*

Suzanne G. E. te Velthuis, Helmut Schultheiss, and Axel Hoffmann

*Materials Science Division, Argonne National Laboratory, Argonne, Illinois 60439, USA*

(Received 7 December 2012; revised manuscript received 29 March 2013; published 6 September 2013)

Strong damping enhancement in nm-thick yttrium iron garnet (YIG) films due to Pt capping layers was observed. This damping is substantially larger than the expected damping due to conventional spin pumping, is accompanied by a shift in the ferromagnetic resonance field, and can be suppressed by the use of a Cu spacer in between the YIG and Pt films. The data indicate that such damping may originate from the ferromagnetic ordering in Pt atomic layers near the YIG/Pt interface and the dynamic exchange coupling between the ordered Pt spins and the spins in the YIG film.

DOI: [10.1103/PhysRevLett.111.106601](https://doi.org/10.1103/PhysRevLett.111.106601)

PACS numbers: 72.25.Mk, 75.70.-i, 76.50.+g

Damping in a magnetic material can be realized through (i) energy redistribution within the magnetic subsystem through magnon-magnon scattering and (ii) energy transfer from the magnetic subsystem to nonmagnetic subsystems such as phonons [1–3]. In a ferromagnetic (FM) film with an adjacent normal metal (NM) film, there exists another damping route—spin pumping, in which magnetization precession in the FM film produces a spin current that flows into the NM film. The process represents a damping fundamentally different from (i) and (ii); it engages energy transfer to an external system, and it is an interface effect and plays an important role only for thin films. Considerable work has been carried out on spin pumping in metallic FM/NM structures since the early 2000s [2,4–7] and recently also in insulating FM/NM systems [8–15].

This Letter reports on experimental evidence for a new damping. The samples consist of nm-thick ferrimagnetic yttrium iron garnet ( $\text{Y}_3\text{Fe}_5\text{O}_{12}$ , YIG) films capped by Pt films. When it is 3 nm or thicker, the Pt layer produces an extra damping that is not only significantly larger than the expected damping from spin pumping ( $\alpha_{\text{sp}}$ ), but is also accompanied by a shift in the ferromagnetic resonance (FMR) field. This damping can be switched off by the addition of a Cu spacer in between the YIG and Pt films. The damping may originate from the FM ordering in the Pt atomic layers near the YIG/Pt interface and the dynamic exchange coupling between the ordered Pt spins and the YIG spins. The FM ordering of the Pt layers is due to the magnetic proximity effect (MPE) [16–22] and has been confirmed by recent x-ray magnetic circular dichroism measurements [23]. The dynamic YIG-Pt coupling allows for the transfer of a part of the damping of the FM Pt to the YIG film.

Because of the presence of the FM Pt, conventional spin pumping from the YIG film to the Pt film does not occur. However, there exists spin pumping from the FM Pt into the paramagnetic (PM) Pt, which contributes to the damping of the FM Pt. The use of a Cu spacer switches off the MPE and thereby turns off the new damping. The damping is denoted as  $\alpha_{\text{MPE}}$  below, as its origin is associated with the MPE.

Three points should be emphasized. (i) Although the results below were obtained with YIG/Pt, one can expect similar results in any systems where the MPE exists, including Ni/Pt [17], NiFe/Pt [21], Fe/Pd [16], NiFe/Pd [20], Fe/W [18], and Fe/Ir [18]. (ii) The new damping cannot be described by existing models [5,8,24] and therefore begs for new theoretical studies on damping in FM/NM systems. (iii) Recently, there appears a research field that uses YIG/Pt structures for spintronics [8–15,22,25–30]. Understanding of damping in YIG/Pt reported below provides significant implications for the future development of this field.

The YIG, YIG/Pt, YIG/Cu, and YIG/Cu/Pt samples were fabricated by pulsed laser deposition (PLD) [31]. The substrates were (111)  $\text{Gd}_3\text{Ga}_5\text{O}_{12}$  wafers with a surface roughness of (0.1–0.2) nm. The YIG/Cu and YIG/Cu/Pt samples where the Cu surfaces are naturally oxidized are denoted as YIG/Cu\* and YIG/Cu\*/Pt, respectively. For these samples, the YIG and Pt layers were grown by PLD, while the Cu layers were deposited by sputtering. Ferromagnetic resonances were measured in microwave shorted waveguides and cavities with in-plane magnetic fields unless otherwise specified, and the FMR linewidths ( $\Delta H$ ) below all refer to the peak-to-peak linewidths of the FMR absorption derivative profiles.

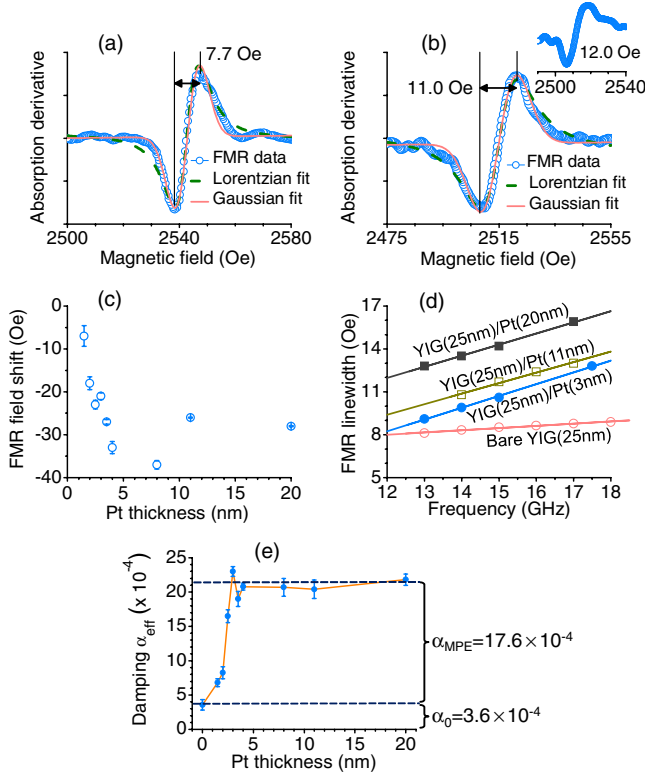


FIG. 1 (color online). (a) FMR profile for a bare YIG (25 nm) sample. (b) FMR profile for a YIG(25 nm)/Pt(20 nm) sample. (c) Pt layer-caused  $H_{\text{FMR}}$  change as a function of the Pt thickness. The data in (a)–(c) were obtained at 9.5 GHz. (d)  $\Delta H$  vs  $\omega/2\pi$  responses for four samples. (e) Damping  $\alpha_{\text{eff}}$  as a function of the Pt thickness.

Figure 1 shows the data for YIG/Pt samples, for which the YIG thickness ( $d_{\text{YIG}}$ ) is 25 nm while the Pt thickness ( $d_{\text{Pt}}$ ) varies in the 0–20 nm range. (a) and (b) The FMR profiles for a bare YIG sample and a YIG/Pt(20 nm) sample, respectively. The circles show the data, while the dashed and solid curves show Lorentzian and Gaussian fits, respectively. (c) The Pt-caused shift of the FMR field ( $H_{\text{FMR}}$ ) as a function of  $d_{\text{Pt}}$ . The data in (a)–(c) were obtained with a 9.5 GHz cavity. The inset in (b) shows an FMR profile measured with a shorted waveguide for the sample cited for the data in (b). These data indicate the consistency of the FMR measurements with a shorted waveguide and a cavity. The difference in  $\Delta H$  for two approaches is usually less than 10%. In (c), each point shows the averaged value over 5–10 measurements, and the error bars show the corresponding standard errors. This is also true for Figs. 2(a), 2(b), 3(a), and 3(b). The symbols in (d) show  $\Delta H$  as a function of microwave frequency ( $\omega/2\pi$ ) for four samples. The solid lines show fits with [32]

$$\sqrt{3}\Delta H = \frac{2\alpha_{\text{eff}}}{|\gamma|} \frac{\omega}{2\pi} + \Delta H_0, \quad (1)$$

where  $\alpha_{\text{eff}}$  is the effective damping parameter,  $|\gamma| = 2.8$  MHz/Oe is the gyromagnetic ratio, and  $\Delta H_0$  denotes

inhomogeneity line broadening. (e)  $\alpha_{\text{eff}}$  as a function of  $d_{\text{Pt}}$ . The  $\alpha_{\text{eff}}$  values were obtained from the fitting of the  $\Delta H-(\omega/2\pi)$  responses with Eq. (1), as shown in (d). The error bars give the standard errors in the fitting. In (e), the components of  $\alpha_{\text{eff}}$  are also given.  $\alpha_0$  was the damping of the bare YIG and  $\alpha_{\text{MPE}}$  was determined as  $\alpha_{\text{MPE}} = \alpha_{\text{eff}} - \alpha_0$ .

The following results are evident from Figs. 1(a)–1(d). The growth of a Pt layer leads to a decrease in  $H_{\text{FMR}}$ , as shown in (a)–(c). The Pt layer also results in an increase in  $\Delta H$ , as shown in (a), (b), and (d).  $\Delta H$  contains a contribution from inhomogeneity, as indicated by the following facts: (i) for the fittings in (a) and (b) the Gaussian functions fit slightly better than the Lorentzian functions; and (ii) the linear fits in (d) all yield nonzero  $\Delta H_0$ . Note that the linear fitting conducted to determine the  $\alpha_{\text{eff}}$  values in Figs. 1 and 2 indicates that  $\Delta H_0$  generally decreases with the sample size and is less than 3 Oe for samples not larger than 2 mm  $\times$  2 mm.

Figure 1(e) shows three results. First, the Pt layer leads to a substantial increase in damping. This increase is consistent with the above-mentioned increase in  $\Delta H$ . Second, the  $\alpha_{\text{eff}}-d_{\text{Pt}}$  response shows a saturation. When  $d_{\text{Pt}} < 3$  nm,  $\alpha_{\text{eff}}$  increases with  $d_{\text{Pt}}$ ; when  $d_{\text{Pt}} \geq 3$  nm,  $\alpha_{\text{eff}}$  is relatively constant. This  $d_{\text{Pt}}$  dependence is similar to that in (c). Third,  $\alpha_{\text{MPE}}$  is substantially larger than spin-pumping damping expected for YIG/NM, which is  $\alpha_{\text{sp}} = 6.9 \times 10^{-4}$ . This damping was calculated by

$$\alpha_{\text{sp}} = \frac{g\mu_B}{4\pi M_s} g_{\parallel} \frac{1}{d_{\text{YIG}}}, \quad (2)$$

where  $g = 2.02$  is the Landau factor,  $\mu_B = 9.274 \times 10^{-21}$  erg/G is the Bohr magneton,  $4\pi M_s = 1300$  G is the saturation induction measured by SQUID, and  $g_{\parallel} = 1.2 \times 10^{14}$  cm $^{-2}$  is the spin mixing conductance [11]. Note that the Pt thickness at which the  $\alpha_{\text{eff}}$  and  $H_{\text{FMR}}$  shift saturate is close to the length scale for the dependence of  $g_{\parallel}$  on  $d_{\text{Pt}}$  for NiFe/Pt [33].

The above results are believed to derive from the FM ordering of spins in Pt atomic layers in the proximity of the YIG film [16–23] and the interfacial coupling between the FM Pt and the YIG film. There exist static and dynamic exchange couplings. The static coupling results in a torque on the YIG magnetization ( $\mathbf{M}$ ) that is proportional to  $\mathbf{M}$  and manifests itself as a shift in  $H_{\text{FMR}}$ . The dynamic coupling also results in a torque, but it is proportional to  $\partial\mathbf{M}/\partial t$  and plays a role of an additional damping [34]. Via this torque, the FM Pt shares its damping with the YIG film, resulting in  $\alpha_{\text{MPE}}$ . This interpretation is supported by the fact that both the “ $H_{\text{FMR}}$  shift- $d_{\text{Pt}}$ ” and “ $\alpha_{\text{eff}}-d_{\text{Pt}}$ ” responses show saturation behavior at  $d_{\text{Pt}} \approx 3$  nm. In more detail, as the Pt film evolves from clusters to a continuous epitaxial film, the interfacial coupling becomes stronger and both the  $H_{\text{FMR}}$  shift and  $\alpha_{\text{eff}}$  increase. When  $d_{\text{Pt}} > 3$  nm, however, the growth of additional Pt leads to

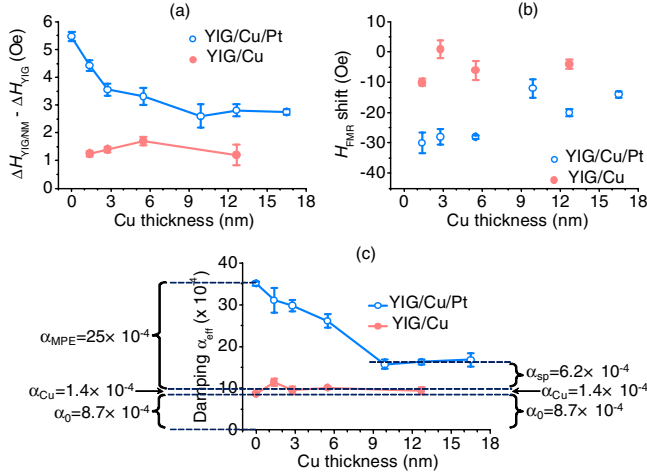


FIG. 2 (color online). Data obtained for YIG(35 nm)/Cu/Pt(23 nm) (empty circles) and YIG(35 nm)/Cu (solid circles). (a) NM layer-caused  $\Delta H$  change as a function of  $d_{\text{Cu}}$ . (b) NM layer-caused  $H_{\text{FMR}}$  change as a function of  $d_{\text{Cu}}$ . (c) Effective damping as a function of  $d_{\text{Cu}}$ .

no further enhancement in interfacial coupling, and the  $H_{\text{FMR}}$  shift and the  $\alpha_{\text{eff}}$  saturate. Since the Pt atomic layers near the YIG/Pt interface are ferromagnetic, conventional spin pumping directly from the interface is not applicable and one has  $\alpha_{\text{sp}} = 0$  and  $\alpha_{\text{eff}} = \alpha_0 + \alpha_{\text{MPE}}$ .

To test the above interpretation, the effects of adding a Cu spacer were studied. Cu was chosen because it has a very weak spin-orbit interaction and a very long spin diffusion length ( $\lambda_d$ ) [35] in comparison with Pt. With an increase in the Cu thickness ( $d_{\text{Cu}}$ ), one can expect a weaker MPE and corresponding decreases in both the  $H_{\text{FMR}}$  shift and  $\alpha_{\text{MPE}}$ . Also, one can expect spin pumping at the YIG/Cu interface and the presence of  $\alpha_{\text{sp}}$ . If  $d_{\text{Cu}} \ll \lambda_d$ , the spin current undergoes weak dissipation in the Cu spacer but flows into and dissipates in the Pt film. Thus, one can expect a very weak dependence of  $\alpha_{\text{sp}}$  on  $d_{\text{Cu}}$  if  $d_{\text{Cu}} \ll \lambda_d$ . For YIG/Cu\*/Pt samples, however, one can expect the Cu oxide not only eliminates  $\alpha_{\text{MPE}}$  and  $H_{\text{FMR}}$  shift, but also prohibits spin pumping.

Figure 2 gives data for YIG(35 nm)/Cu and YIG(35 nm)/Cu/Pt(23 nm), for which  $d_{\text{Cu}}$  varies in the 0–17 nm range. (a) and (b) give 9.5-GHz FMR data. (a) gives the NM-caused change in  $\Delta H$  as a function of  $d_{\text{Cu}}$ , while (b) gives the  $H_{\text{FMR}}$  shift as a function of  $d_{\text{Cu}}$ . (c) presents  $\alpha_{\text{eff}}$  as a function of  $d_{\text{Cu}}$  as well as the components of  $\alpha_{\text{eff}}$ . The data for the YIG/Cu samples indicate that the growth of a Cu layer yields an extra damping ( $\alpha_{\text{Cu}}$ ) much smaller than  $\alpha_0$ . This agrees with the expectation that a NM capping layer should not change the relaxation in the YIG film in the absence of the MPE and spin pumping. The spin pumping is absent because  $d_{\text{Cu}} \ll \lambda_d$  [35]. This is supported by the fact that the YIG/Cu samples show very similar  $\alpha_{\text{eff}}$  values in spite of a relatively wide  $d_{\text{Cu}}$  range (0–12.7 nm). If spin pumping at the YIG/Cu

interfaces makes significant contributions to  $\alpha_{\text{eff}}$ , one would expect that  $\alpha_{\text{eff}}$  increases with  $d_{\text{Cu}}$  [5]. Although  $\alpha_{\text{Cu}}$  is small, its presence might indicate that the process of the Cu growth slightly enhances the imperfection on the YIG surface, which yields a damping enhancement.

The data for YIG/Cu/Pt indicate that a Cu spacer can reduce the  $H_{\text{FMR}}$  shift,  $\Delta H$ , and  $\alpha_{\text{eff}}$  in YIG/Pt. Moreover, the thicker the Cu spacer is, the larger the reductions are. One also sees that for the samples with  $d_{\text{Cu}} \geq 10$  nm, an additional increase in  $d_{\text{Cu}}$  does not result in a further reduction in  $\alpha_{\text{eff}}$ . This indicates that the YIG/Cu( $\geq 10$  nm)/Pt samples have  $\alpha_{\text{MPE}} = 0$  and  $\alpha_{\text{eff}} = \alpha_0 + \alpha_{\text{Cu}} + \alpha_{\text{sp}}$ . Thus, one has  $\alpha_{\text{sp}} = \alpha_{\text{eff}} - \alpha_0 - \alpha_{\text{Cu}} = 6.2 \times 10^{-4}$  for YIG/Cu( $\geq 10$  nm)/Pt. Assuming that the growth of a Pt capping layer also slightly modifies the YIG surface and yields a small damping enhancement as the growth of a Cu layer does, one can then determine  $\alpha_{\text{MPE}}$  in YIG(35 nm)/Pt(23 nm) as  $\alpha_{\text{MPE}} = \alpha_{\text{eff}} - \alpha_0 - \alpha_{\text{Cu}}$ , which is given in (c). One can see that  $\alpha_{\text{MPE}}$  is notably larger than  $\alpha_0$  and  $\alpha_{\text{sp}}$ , similar to the results indicated by the data in Fig. 1(e).

Consider now YIG/Cu\*/Pt for which the data are shown in Fig. 3. The NM-caused changes in  $\Delta H$  and  $H_{\text{FMR}}$ , respectively, as a function of the Cu\* thickness ( $d_{\text{Cu}^*}$ ) are shown in (a) and (b). The data were measured at 9.5 GHz. (c)–(f) give the  $\Delta H$ –( $\omega/2\pi$ ) responses for four samples. The open circles show the data from in-plane FMR measurements, while the solid circles show those obtained with out-of-plane fields. In (c)–(f), the lines show the fits with Eq. (1). The  $\alpha_{\text{eff}}$  values from the fitting are given in Table I.

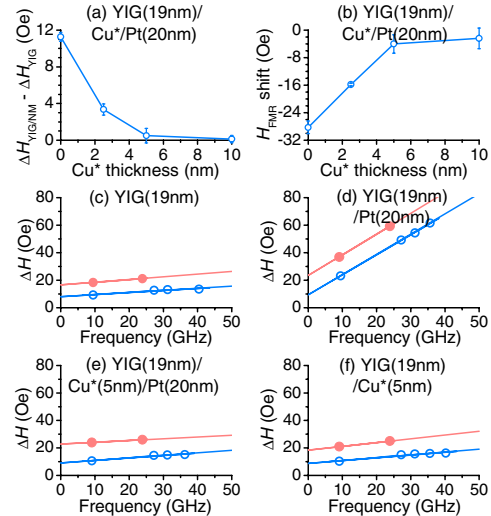


FIG. 3 (color online). Data obtained for YIG(19 nm)/Cu\*/Pt(20 nm) samples as well as several control YIG samples. (a) NM layer-caused  $\Delta H$  change as a function of the Cu thickness ( $d_{\text{Cu}^*}$ ). (b) NM layer-caused  $H_{\text{FMR}}$  shift. (c)–(f)  $\Delta H$  as a function of frequency for four samples. The open and solid circles show the data from in-plane and out-of-plane FMR measurements, respectively.

TABLE I. Effective damping parameters.

| Sample                             | $\alpha_{\text{eff}} (\times 10^{-4})$<br>(in plane) | $\alpha_{\text{eff}} (\times 10^{-4})$<br>(out-of-plane) |
|------------------------------------|--|--|
| YIG(19 nm)                         | $3.58 \pm 0.76$                                      | 4.72   |
| YIG(19 nm)/Pt(20 nm)               | $35.36 \pm 0.58$                                     | 36.60  |
| YIG(19 nm)/Cu*(5 nm)/<br>Pt(20 nm) | $4.33 \pm 0.58$                                      | 3.41   |
| YIG(19 nm)/Cu*(5 nm)               | $4.82 \pm 0.62$                                      | 6.71   |

Three results are evident from Fig. 3 and Table I. The Pt-caused additional damping is substantially larger than  $\alpha_0$  and  $\alpha_{\text{sp}}$ . In contrast to the situation for YIG/Cu/Pt, a 5-nm-thick Cu\* spacer is sufficient to suppress both  $\alpha_{\text{MPE}}$  and the  $H_{\text{FMR}}$  shift. This is indicated by the fact that the  $\Delta H$  values for YIG/Cu\*(5 nm)/Pt and YIG/Cu\*(10 nm)/Pt almost match that of the bare YIG sample, as shown in (a), and the  $H_{\text{FMR}}$  shifts for YIG/Cu\*(5 nm)/Pt and YIG/Cu\*(10 nm)/Pt are close to zero, as shown in (b). There is no evidence of spin pumping in YIG/Cu\*/Pt, as indicated by the fact that the  $\alpha_{\text{eff}}$  values of YIG/Cu\*(5 nm) and YIG/Cu\*(5 nm)/Pt are very close to each other and are also close to  $\alpha_0$  (see Table I). Note that although the out-of-plane FMR measurements were carried out at two frequencies only, the  $\alpha_{\text{eff}}$  values obtained from the fitting are all close to those obtained from in-plane FMR measurements. This closeness assures the accuracy of the damping values presented. It also indicates that two-magnon scattering makes small contributions to  $\alpha_0$ .

The results from Figs. 2 and 3 confirm the presence of  $\alpha_{\text{MPE}}$  in YIG/Pt. Moreover, they verify the above-discussed expectations: a Cu spacer can decouple the YIG and Pt films and thereby suppress both the  $H_{\text{FMR}}$  shift and  $\alpha_{\text{MPE}}$ , and the Cu spacer facilitates the spin pumping of the YIG film in the absence of Cu surface oxidation but does not in the presence of Cu surface oxidation. The results, therefore, support the interpretation on the origin of  $\alpha_{\text{MPE}}$ .

The data in Figs. 2 and 3 also indicate incomplete decoupling between the YIG and Pt films in YIG/Cu(<10 nm)/Pt and YIG/Cu\*(<5 nm)/Pt. The decoupling is incomplete because the YIG films have relatively large roughness. For a YIG film with a much smoother surface, one can expect complete decoupling as well as the complete suppression of  $\alpha_{\text{MPE}}$  with a thinner Cu spacer ( $d_{\text{Cu}} < 10$  nm,  $d_{\text{Cu}^*} < 5$  nm). Figure 4 gives atomic force microscopy images of three samples. One can see that the YIG/Cu interface has a large roughness, while the Cu/Pt interface is relatively smooth. Because of this, it is conceivable that there are local regions in YIG/Cu/Pt where the YIG-to-Pt distance is much smaller than the nominal Cu thickness.

Mizukami *et al.* observed the decrease of damping in NiFe/Cu/Pt with  $d_{\text{Cu}}$  and a saturation in the damping

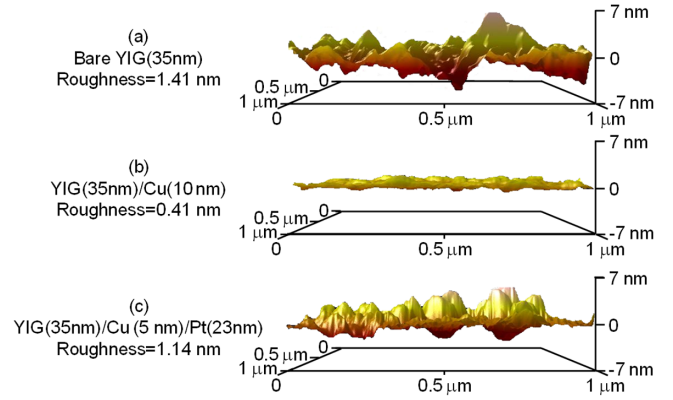


FIG. 4 (color online). Atomic force microscopy surface images of three samples.

reduction at  $d_{\text{Cu}} = 200\text{--}300$  nm [5]. They explained the results with a model based on the spin diffusion in Cu. This model is not applicable to this work because  $d_{\text{Cu}} \ll \lambda_d$ . Rezende *et al.* proposed a model to explain large dampings in  $\mu\text{m}$ -thick YIG films with Pt capping layers [24]. The model yields a damping independent of  $d_{\text{YIG}}$  and is therefore inconsistent with the above-discussed interpretation. Furthermore, Kajiwara *et al.* developed a model for spin pumping at YIG/Pt interfaces, which, however, did not consider the MPE [8].  $\alpha_{\text{MPE}}$  is expected to scale with  $1/d_{\text{YIG}}$ . However, this scaling is not shown by the above-presented data, although YIG(19 nm)/Pt shows much larger  $\alpha_{\text{MPE}}$  than YIG(25 nm)/Pt and YIG(35 nm)/Pt. This is because  $\alpha_{\text{MPE}}$  also depends on the properties of the particular YIG/Pt interface. One can also expect a larger  $H_{\text{FMR}}$  shift in YIG/Pt structures with much thinner YIG films and insignificant shifts in structures with much thicker YIG films. The latter was reported recently [15,24].

Consider finally spin pumping from the FM Pt to the PM Pt. Recent calculations show that the MPE causes the ordering of four Pt atomic layers near the YIG/Pt interface [36]. The effective thickness of the ordered layers ( $d_{\text{FM-Pt}}$ ) is 0.96 nm. Since  $d_{\text{FM-Pt}}$  is much smaller than  $d_{\text{YIG}}$ , one can assume that the contribution from the intrinsic damping of the FM Pt to  $\alpha_{\text{MPE}}$  is very small, and  $\alpha_{\text{sp}}$  due to pumping from the FM Pt to the PM Pt dominates  $\alpha_{\text{MPE}}$ . Thus, one can estimate  $g_{\uparrow\downarrow}$  at the FM Pt/PM Pt interface by

$$\alpha_{\text{MPE}} \approx \frac{g_{\uparrow\downarrow} \mu_B g_{\uparrow\downarrow}}{4\pi M_s d_{\text{YIG}} + 4\pi M_{\text{FM-Pt}} d_{\text{FM-Pt}}} \quad (3)$$

where  $4\pi M_{\text{FM-Pt}} = 90$  G [36]. Taking the data in Table I, one obtains  $g_{\uparrow\downarrow} \approx 4.2 \times 10^{14} \text{ cm}^{-2}$ , which is larger than that at YIG/Au [11] or YIG/Cu [37] interfaces.

This work was supported in part by U.S. National Science Foundation (No. ECCS-1231598), the U.S. Army Research Office (No. W911NF-12-1-0518, No. W911NF-11-C-0075), the U.S. National Institute of Standards and Technology (No. 60NANB10D011), the

U.S. Department of Energy, Office of Basic Energy Sciences (No. DE-AC02-06CH11357), the Natural Sciences and Engineering Research Council of Canada, and the Canadian Institute for Advanced Research.

\*Corresponding author.

mwu@lamar.colostate.edu

- [1] M. Sparks, *Ferromagnetic-Relaxation Theory* (McGraw-Hill, New York, 1964).
- [2] B. Heinrich and J.A.C. Bland, *Ultrathin Magnetic Structures: Fundamentals of Nanomagnetism* (Springer, Berlin, 2005).
- [3] R.D. McMichael and P. Krivosik, *IEEE Trans. Magn.* **40**, 2 (2004).
- [4] R. Urban, G. Woltersdorf, and B. Heinrich, *Phys. Rev. Lett.* **87**, 217204 (2001).
- [5] S. Mizukami, Y. Ando, and T. Miyazaki, *Phys. Rev. B* **66**, 104413 (2002).
- [6] Y. Tserkovnyak, A. Brataas, and G.E.W. Bauer, *Phys. Rev. Lett.* **88**, 117601 (2002).
- [7] B. Heinrich, Y. Tserkovnyak, G. Woltersdorf, A. Brataas, R. Urban, and G.E.W. Bauer, *Phys. Rev. Lett.* **90**, 187601 (2003).
- [8] Y. Kajiwara, K. Harii, S. Takahashi, J. Ohe, K. Uchida, M. Mizuguchi, H. Umezawa, H. Kawai, K. Ando, K. Takanashi, S. Maekawa, and E. Saitoh, *Nature (London)* **464**, 262 (2010).
- [9] C.W. Sandweg, Y. Kajiwara, K. Ando, E. Saitoh, and B. Hillebrands, *Appl. Phys. Lett.* **97**, 252504 (2010).
- [10] C.W. Sandweg, Y. Kajiwara, A.V. Chumak, A.A. Serga, V.I. Vasyuchka, M.B. Jungfleisch, E. Saitoh, and B. Hillebrands, *Phys. Rev. Lett.* **106**, 216601 (2011).
- [11] B. Heinrich, C. Burrowes, E. Montoya, B. Kardasz, E. Girt, Y.-Y. Song, Y. Sun, and M. Wu, *Phys. Rev. Lett.* **107**, 066604 (2011).
- [12] H. Kurebayashi, O. Dzyapko, V.E. Demidov, D. Fang, A.J. Ferguson, and S.O. Demokritov, *Nat. Mater.* **10**, 660 (2011).
- [13] L.H. Vilela-Leão, C. Salvador, A. Azevedo, and S.M. Rezende, *Appl. Phys. Lett.* **99**, 102505 (2011).
- [14] C. Burrowes, B. Heinrich, B. Kardasz, E.A. Montoya, E. Girt, Y. Sun, Y.-Y. Song, and M. Wu, *Appl. Phys. Lett.* **100**, 092403 (2012).
- [15] V. Castel, N. Vlietstra, J. Ben Youssef, and B.J. van Wees, *Appl. Phys. Lett.* **101**, 132414 (2012).
- [16] E.E. Fullerton, D. Stoeffler, K. Ounadjela, B. Heinrich, Z. Celinski, and J.A.C. Bland, *Phys. Rev. B* **51**, 6364 (1995).
- [17] F. Wilhelm, P. Pouloupoulos, G. Ceballos, H. Wende, K. Baberschke, P. Srivastava, D. Benea, H. Ebert, M. Angelakeris, N.K. Flevaris, D. Niarchos, A. Rogalev, and N.B. Brookes, *Phys. Rev. Lett.* **85**, 413 (2000).
- [18] F. Wilhelm, P. Pouloupoulos, H. Wende, A. Scherz, and K. Baberschke, M. Angelakeris, N.K. Flevaris, and A. Rogalev, *Phys. Rev. Lett.* **87**, 207202 (2001).
- [19] F. Wilhelm, M. Angelakeris, N. Jaouen, P. Pouloupoulos, E.Th. Papaioannou, Ch. Mueller, P. Fumagalli, A. Rogalev, and N.K. Flevaris, *Phys. Rev. B* **69**, 220404(R) (2004).
- [20] W.E. Bailey, A. Ghosh, S. Auffret, E. Gautier, U. Ebels, F. Wilhelm, and A. Rogalev, *Phys. Rev. B* **86**, 144403 (2012).
- [21] W.L. Lim, N. Ebrahim-Zadeh, J.C. Owens, H.G.E. Hentschel, and S. Urazhdin, *Appl. Phys. Lett.* **102**, 162404 (2013).
- [22] S.Y. Huang, X. Fan, D. Qu, Y.P. Chen, W.G. Wang, J. Wu, T.Y. Chen, J.Q. Xiao, and C.L. Chien, *Phys. Rev. Lett.* **109**, 107204 (2012).
- [23] Y.M. Lu, Y. Choi, C.M. Ortega, X.M. Cheng, J.W. Cai, S.Y. Huang, L. Sun, and C.L. Chien, *Phys. Rev. Lett.* **110**, 147207 (2013).
- [24] S.M. Rezende, R. Rodríguez-Suárez, M.M. Soares, L.H. Vilela-Leão, and A. Azevedo, *arXiv:1207.3330v1*.
- [25] K. Uchida, J. Xiao, H. Adachi, J. Ohe, S. Takahashi, J. Ieda, T. Ota, Y. Kajiwara, H. Umezawa, H. Kawai, G.E.W. Bauer, S. Maekawa, and E. Saitoh, *Nat. Mater.* **9**, 894 (2010).
- [26] J. Xiao, G.E.W. Bauer, K.-C. Uchida, E. Saitoh, and S. Maekawa, *Phys. Rev. B* **81**, 214418 (2010).
- [27] M.B. Jungfleisch, A.V. Chumak, V.I. Vasyuchka, A.A. Serga, B. Obry, H. Schultheiss, P.A. Beck, A.D. Karenowska, E. Saitoh, and B. Hillebrands, *Appl. Phys. Lett.* **99**, 182512 (2011).
- [28] E. Padrón-Hernández, A. Azevedo, and S.M. Rezende, *Phys. Rev. Lett.* **107**, 197203 (2011).
- [29] E. Padrón-Hernández, A. Azevedo, and S.M. Rezende, *Appl. Phys. Lett.* **99**, 192511 (2011).
- [30] A.V. Chumak, A.A. Serga, M.B. Jungfleisch, R. Neb, D.A. Bozhko, V.S. Tiberkevich, and B. Hillebrands, *Appl. Phys. Lett.* **100**, 082405 (2012).
- [31] Y. Sun, Y.-Y. Song, H. Chang, M. Kabatek, M. Jantz, W. Schneider, M. Wu, H. Schultheiss, and A. Hoffmann, *Appl. Phys. Lett.* **101**, 152405 (2012).
- [32] S.S. Kalarickal, P. Krivosik, J. Das, K.S. Kim, and C.E. Patton, *Phys. Rev. B* **77**, 054427 (2008).
- [33] Z. Feng, J. Hu, L. Sun, B. You, D. Wu, J. Du, W. Zhang, A. Hu, Y. Yang, D.M. Tang, B.S. Zhang, and H.F. Ding, *Phys. Rev. B* **85**, 214423 (2012).
- [34] B. Heinrich and J.F. Cochran, *Adv. Phys.* **42**, 523 (1993).
- [35] T. Kimura, J. Hamrle, and Y. Otani, *Phys. Rev. B* **72**, 014461 (2005).
- [36] D. Qu, S.Y. Huang, J. Hu, R. Wu, and C.L. Chien, *Phys. Rev. Lett.* **110**, 067206 (2013).
- [37] Y. Sun and M. Wu, “Yttrium Iron Garnet Nano Films: Epitaxial Growth, Spin Pumping Efficiency, and Platinum Capping-Caused Damping,” in *Solid State Physics Vol. 64*, edited by M. Wu and A. Hoffmann (Elsevier, London, to be published).